IEICE TRANS. ELECTRON., VOL.E105–C, NO.4 APRIL 2022

BRIEF PAPER *Special Section on Recent Progress in Electromagnetic Theory and Its Application*

Numerical Analysis of Pulse Response for Slanted Grating Structure with an Air Regions in Dispersion Media by TE Case

Ryosuke OZAKI[†a)], ***Member and*** **Tsuneki YAMASAKI**[†], ***Senior Member***

SUMMARY In our previous paper, we have proposed a new numerical technique for transient scattering problem of periodically arrayed dispersion media by using a combination of the fast inversion Laplace transform (FILT) method and Fourier series expansion method (FSEM), and analyzed the pulse response for several widths of the dispersion media or rectangular cavities. From the numerical results, we examined the influence of a periodically arrayed dispersion media with a rectangular cavity on the pulse response. In this paper, we analyzed the transient scattering problem for the case of dispersion media with slanted air regions by utilizing a combination of the FILT, FSEM, and multilayer division method (MDM), and investigated an influence for the slanted angle of an air region. In addition, we verified the computational accuracy for term of the MDM and truncation mode number of the electromagnetic fields.

key words: *pulse response, slanted air region, multilayer division method, FILT method, FSEM*

1. Introduction

Recently, the environment problem for global warming phenomenon is very serious challenges such as large scale flood damage caused by guerrilla rainstorm in the world. In addition, the deterioration of a building for tunnel or the road is became social issues. As one of the reasons for these problems, we can consider that it is damage to buried pipes in underground structures or the formation of cavities due to the seepage of rainwater into the underground [1]. On the other hand, the ground penetrating radar (GPR) [2], [3] is generally known as a technology which can explore subsurface structures. The GPR is used such as exploration of rebar structure, metal or landmine detections [4], archaeological and geological surveys in a wide range of these fields, and in relatively shallow underground structures under concrete. In particular, the GPR is well known as useful tool and technology that measures the behavior of a wave reflected by target objects in subsurface structure [5]–[8]. As we are required to explore the target objects buried in subsurface structure without destroying [9], it is important to check whether buried objects are damaged by regular maintenance and inspections. In general, the electric constant is a function of frequency in a medium of the subsurface structures. Therefore, it is necessary to treat the ground as dispersion medium. Furthermore, it needs to consider the inhomogeneous media for the case of arbitrary cavity regions in underground medium. From above explanation, these problems are known as inverse scattering problem in the fields of the electromagnetic field theory. The finite difference time domain (FDTD) method is used to analyze the transient scattering problem caused by cavity under reinforced concrete and circular pipes buried in underground [4], [7], [10]–[12]. But in general, the medium constants in soil are expressed a complex dielectric constant. And so, they have not been analyzed by using the complex dielectric constant with a function of frequency in dispersion medium in detail. However, nowadays, the inverse scattering problem of the electromagnetic waves has become of interest for remote sensing and further development of imaging technology [13], [14].

In our previous paper [15], we proposed a method for determining soil electromagnetic parameters which matched experimentally obtained values [16], and investigated the fundamental problem of dispersion medium with reflective plate based on resulting waveform. Then, we analyzed the pulse response with periodically conducting strips in dispersion media by utilizing a combination of the point matching method (PMM) [17] and the fast inversion of Laplace transform (FILT) method [18]–[20], and investigated the effect of conducting strips and those widths from difference waveform [21], [22]. In recent paper [23], we also have reported the distribution of electric field based on the resulting waveform as first investigation of imaging technology. Furthermore, in order to analyze the dispersion media with inhomogeneous property, we have investigated the transient scattering problem of periodically arrayed dispersion media with rectangular air region by using a combination of the Fourier series expansion method (FSEM) and the FILT method [24]. As reason for dealing with the periodic structure, if the periodic length of the periodic structure is increased, this structure can be approximated to the problem in regard to general remote sensing for the single object buried in subsurface structures.

In this paper, we analyze the transient scattering problem for slanted grating structure [25]–[30] periodically arrayed with cavity and dispersion medium as the first step of an arbitrary cavity shape by using a combination of the FSEM, FILT method, and multilayer division method (MDM) [31], [32], and investigate an influence of slanted air widths from resulting waveform. The background and motivation of incorporating with the MDM are as follows: (1) Establishment of analysis method applicable to problem which is buried in arbitrary object in the future. (2) All elec-

Manuscript received April 11, 2021.
Manuscript revised July 30, 2021.
Manuscript publicized October 18, 2021.

[†]The authors are with Department of Electrical Engineering, College of Science and Technology, Nihon University, Tokyo, 101–8308 Japan.
a) E-mail: ozaki.ryousuke@nihon-u.ac.jp

DOI: 10.1587/transele.2021RES0001

Copyright © 2022 The Institute of Electronics, Information and Communication Engineers

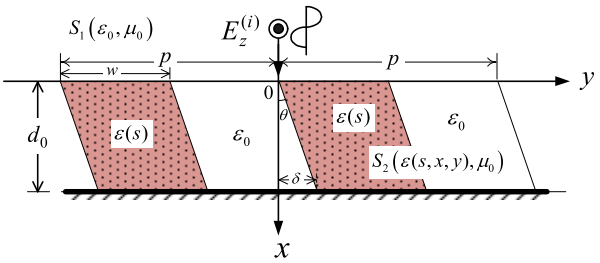

Fig. 1 Structure of slanted grating with air region in dispersion media

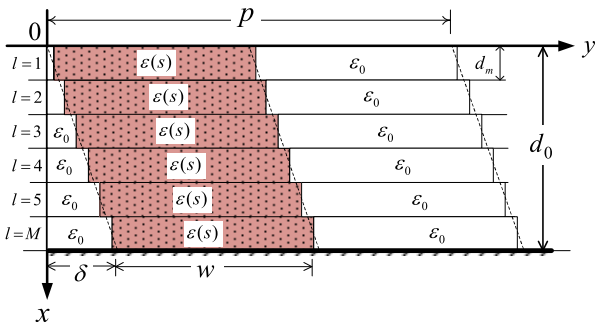

Fig. 2 Multilayer division method in dispersion medium for $M = 6$

tromagnetic fields can be obtained from the electromagnetic field of the first layer in slanted grating structure. (3) The number of dimension for simultaneous equation to be solved does not depend on the number of layers even in time response analysis.

Moreover, we verified the accuracy of the MDM and truncation mode number of the electromagnetic field. From the above investigation, we clarified the validity of present method in complex frequency domain.

2. Method of Analysis

We consider the slanted grating structure with air region in dispersion media as shown in Fig. 1. The structure is uniform in the z-direction, and is periodic length p in the y-direction. To examine an influence for basic response waveform and effectiveness of our numerical technique, we embedded with reflective plate at $x = d_0$. The permittivity of region S_1 ($x \le 0$) is dielectric constant ε_0, that of region S_2 ($0 < x \le d_0$) is complex dielectric constant $\varepsilon(s,x,y)$ in one period. The permeability is assumed to be μ_0 in all regions. Here, the width of dispersion medium is w, and the slanted angle θ is defined as $\tan^{-1}(\delta/d_0)$, and also δ is the slanted width. The time dependence of the electromagnetic fields is $\exp(st)$ in complex frequency domain and is omitted in the field expression.

In the formulation, the TE (the electric field has only the y-component) case is discussed, the notation of the electromagnetic field in the time domain are denoted by $\boldsymbol{E}$ and $\boldsymbol{H}$, while those in the complex frequency domain by $\widetilde{\boldsymbol{E}}$ and $\widetilde{\boldsymbol{H}}$.

When the sine pulse is assumed to be normal incidence from $x < 0$, the electric field in region S_1 is expressed as

$$\widetilde{E}_z^{(1)}(x,y) = \widetilde{E}_z^{(i)}(x) + \widetilde{E}_z^{(r)}(x,y), \tag{1}$$

$$= \widetilde{E}_0^{(i)} e^{-sx/c} + \sum_{n=-N_1}^{N_1} R_n e^{\tilde{k}_1^{(n)} x - j\frac{2n\pi}{p}y}, \tag{2}$$

$$\widetilde{H}_y^{(r)}(x,y) = \frac{1}{s\mu_0}\sum_{n=-N_1}^{N_1} \tilde{k}_1^{(n)} R_n e^{\tilde{k}_1^{(n)} x - j\frac{2n\pi}{p}y}, \tag{3}$$

$$\widetilde{E}_0^{(i)} = \frac{(2\pi/t_w)}{s^2 + (2\pi/t_w)^2}\left(1 - e^{-t_w s}\right), \quad k_0 \triangleq s\sqrt{\varepsilon_0\mu_0} = s/c,$$

$$\tilde{k}_1^{(n)} \triangleq \sqrt{\tilde{k}_0^2 - (-j2n\pi/p)^2},$$

where $\widetilde{E}_0^{(i)}$ is image function of sine pulse at $x = 0$, t_w is pulse width of incident pulse, $\tilde{k}_1^{(n)}$ is the propagation constants in the x-direction, $\tilde{k}_0$ is the wave number in free space, and c is the light velocity.

In the slanted region S_2 ($0 < x \le d_0$), we employ the multilayer division method (MDM). The slanted region is divided into thin layers of M layer and the permittivity distribution $\varepsilon^{(l)}(s,x,y)$ in each layer is approximated by step index profile in the y-direction as shown in Fig. 2. In order to derive the electromagnetic fields in each layer, we express by using the eigenvalues and eigenvector obtained from the following eigenvalue equation:

$$\boldsymbol{\Lambda}\boldsymbol{U}_n^{(l)} = \{\tilde{h}^{(l)}\}^2 \boldsymbol{U}_n^{(l)}, \tag{4}$$

where,

$$\boldsymbol{U}_n^{(l)} \triangleq [\tilde{u}_{-N_1}^{(l)}, \cdots, \tilde{u}_0^{(l)}, \cdots, \tilde{u}_{+N_1}^{(l)}]^T,\ T\text{: Transpose},$$

$$\boldsymbol{\Lambda} \triangleq [\tilde{\zeta}_{n,m}^{(l)}],\ -N_1 \le m \le N_1,\ l = 1 \sim M,$$

$$\tilde{\zeta}_{n,m}^{(l)} \triangleq \tilde{k}_0^2 \tilde{\eta}_{n,m}^{(l)} + \left(\frac{2n\pi}{p}\right)^2,\ -N_1 \le n \le N_1,$$

$$\tilde{\eta}_{n,m}^{(l)} \triangleq \frac{1}{p}\int_0^p \left(\frac{\varepsilon^{(l)}(s,x,y)}{\varepsilon_0}\right) e^{-j\frac{2(n-m)\pi}{p}y} dy.$$

However, the solutions of Eq. (4) in M layer are derived by shifting the first layer profile as following relation [25]:

$$\tilde{h}_\nu^{(l)} = \tilde{h}_\nu^{(1)},\ \tilde{u}_{\nu,n}^{(l)} = \tilde{u}_{\nu,n}^{(1)} \exp(j2n\pi\delta_l/p), \tag{5}$$

where,

$$\delta_l \triangleq y_l - y_1,\ y_l \triangleq (l - 1/2)d_m \tan(\theta),$$

$$d_m \triangleq d_0/M,\ 1 \le l \le M,\ \nu = 1 \sim (2N_1 + 1).$$

Therefore, the electromagnetic fields of region S_2 can be expanded as following equation:

$$\widetilde{E}_z^{(2,l)}(x,y) = \sum_{\nu=1}^{2N_1+1} [A_\nu^{(l)} e^{-\tilde{h}_\nu^{(l)}\{x-(l-1)d_m\}} + B_\nu^{(l)} e^{\tilde{h}_\nu^{(l)}(x-ld_m)}]\, \tilde{f}_\nu^{(l)}(y), \tag{6}$$

$$\tilde{f}_\nu^{(l)}(y) \triangleq \sum_{n=-N_1}^{N_1} \tilde{u}_{\nu,n}^{(l)}\, e^{-j\frac{2n\pi}{p}y}, \tag{7}$$

$$\widetilde{H}_y^{(2,l)}(x,y) \triangleq \frac{1}{\mu_0 s}\frac{\partial \widetilde{E}_z^{(2,l)}(x,y)}{\partial x}, \tag{8}$$

where $A_\nu^{(l)}$, $B_\nu^{(l)}$ are unknown coefficients to be determined by boundary conditions. From the boundary conditions at $x = 0$, $x = d_0$, and $x = ld_m$ ($l = 1 \sim (M-1)$), we derive the relational expression of unknown coefficients.

First, by the boundary condition at $x = 0$ and $x = d_0$, we obtain the following equation by matrix algebra:

$$\boldsymbol{Q}_1 \boldsymbol{A}_\nu^{(1)} + \boldsymbol{Q}_2 \boldsymbol{B}_\nu^{(1)} = \boldsymbol{E}_i, \tag{9}$$

$$\boldsymbol{Q}_3 \boldsymbol{A}_\nu^{(M)} + \boldsymbol{Q}_4 \boldsymbol{B}_\nu^{(M)} = \boldsymbol{0}, \tag{10}$$

where,

$$\begin{aligned}
&\boldsymbol{Q}_\kappa \triangleq [\tilde{q}_{\nu,n}^{(\kappa)}],\ \kappa = 1 \sim 4,\\
&\tilde{q}_{\nu,n}^{(1)} \triangleq (\tilde{k}_1^{(n)} + \tilde{h}_\nu^{(1)})\tilde{u}_{\nu,n}^{(1)},\ \tilde{q}_{\nu,n}^{(2)} \triangleq (\tilde{k}_1^{(n)} - \tilde{h}_\nu^{(1)})e^{-\tilde{h}_\nu^{(1)} d_m}\tilde{u}_{\nu,n}^{(1)},\\
&\tilde{q}_{\nu,n}^{(3)} \triangleq e^{-\tilde{h}_\nu^{(M)} d_m}\tilde{u}_{\nu,n}^{(M)},\ \tilde{q}_{\nu,n}^{(4)} \triangleq \tilde{u}_{\nu,n}^{(M)},\\
&\nu = 1 \sim (2N_1+1),\ -N_1 \le n \le N_1,\\
&\boldsymbol{A}_\nu^{(\alpha)} \triangleq [A_1^{(\alpha)}, A_2^{(\alpha)}, \cdots, A_{2N_1+1}^{(\alpha)}]^T,\\
&\boldsymbol{B}_\nu^{(\alpha)} \triangleq [B_1^{(\alpha)}, B_2^{(\alpha)}, \cdots, B_{2N_1+1}^{(\alpha)}]^T,\ \alpha = 1 \text{ or } M,\\
&\boldsymbol{E}_i \triangleq [0, \cdots, (\tilde{k}_0 + \tilde{k}_1^{(0)})\widetilde{E}_0^{(i)}, \cdots, 0].
\end{aligned}$$

Next, we derive the matrix relation between $\boldsymbol{A}_\nu^{(1)}, \boldsymbol{B}_\nu^{(1)}$ and $\boldsymbol{A}_\nu^{(M)}, \boldsymbol{B}_\nu^{(M)}$. By the boundary condition at $x = ld_m$, we can expand as following equation:

$$\begin{aligned}
\begin{pmatrix} \boldsymbol{A}_\nu^{(1)} \\ \boldsymbol{B}_\nu^{(1)} \end{pmatrix} &= \begin{pmatrix} \boldsymbol{G}_1^{(1)} & \boldsymbol{G}_2^{(1)} \\ \boldsymbol{G}_3^{(1)} & \boldsymbol{G}_4^{(1)} \end{pmatrix}\begin{pmatrix} \boldsymbol{G}_1^{(2)} & \boldsymbol{G}_2^{(2)} \\ \boldsymbol{G}_3^{(2)} & \boldsymbol{G}_4^{(2)} \end{pmatrix}\\
&\quad \cdots \begin{pmatrix} \boldsymbol{G}_1^{(M-1)} & \boldsymbol{G}_2^{(M-1)} \\ \boldsymbol{G}_3^{(M-1)} & \boldsymbol{G}_4^{(M-1)} \end{pmatrix}\begin{pmatrix} \boldsymbol{A}_\nu^{(M)} \\ \boldsymbol{B}_\nu^{(M)} \end{pmatrix}\\
&= \begin{pmatrix} \boldsymbol{G}_1 & \boldsymbol{G}_2 \\ \boldsymbol{G}_3 & \boldsymbol{G}_4 \end{pmatrix}\begin{pmatrix} \boldsymbol{A}_\nu^{(M)} \\ \boldsymbol{B}_\nu^{(M)} \end{pmatrix},
\end{aligned} \tag{11}$$

where,

$$\begin{aligned}
&\boldsymbol{G}_\kappa^{(l)} \triangleq [\tilde{g}_{\nu,n}^{(\kappa,l)}],\ \kappa = 1 \sim 4,\ l = 1 \sim (M-1),\\
&\tilde{g}_{\nu,n}^{(1,l)} \triangleq \frac{1}{2}[\tilde{\gamma}_{\nu,n}^{(l)} + \tilde{\gamma}_{\nu,n}^{(l)}\tilde{h}_\nu^{(l+1)}/\tilde{h}_\nu^{(l)}]e^{\tilde{h}_\nu^{(l)} d_m},\\
&\tilde{g}_{\nu,n}^{(2,l)} \triangleq \frac{1}{2}[\tilde{\gamma}_{\nu,n}^{(l)} - \tilde{\gamma}_{\nu,n}^{(l)}\tilde{h}_\nu^{(l+1)}/\tilde{h}_\nu^{(l)}]e^{-(\tilde{h}_\nu^{(l+1)} - \tilde{h}_\nu^{(l)})d_m},\\
&\tilde{g}_{\nu,n}^{(3,l)} \triangleq \frac{1}{2}[\tilde{\gamma}_{\nu,n}^{(l)} - \tilde{\gamma}_{\nu,n}^{(l)}\tilde{h}_\nu^{(l+1)}/\tilde{h}_\nu^{(l)}],\\
&\tilde{g}_{\nu,n}^{(4,l)} \triangleq \frac{1}{2}[\tilde{\gamma}_{\nu,n}^{(l)} + \tilde{\gamma}_{\nu,n}^{(l)}\tilde{h}_\nu^{(l+1)}/\tilde{h}_\nu^{(l)}]e^{-\tilde{h}_\nu^{(l+1)} d_m},\\
&\tilde{\gamma}_{\nu,n}^{(l)} \triangleq [\tilde{u}_{\nu,n}^{(l)}]^{-1} \cdot [\tilde{u}_{\nu,n}^{(l+1)}],\\
&\qquad \nu = 1 \sim (2N_1+1),\ -N_1 \le n \le N_1.
\end{aligned}$$

Rearranging Eqs. (9), (10), (11) with respect to $\boldsymbol{A}_\nu^{(M)}$, we can get the simultaneous equation by matrix algebra as follows:

$$\boldsymbol{X} \cdot \boldsymbol{A}_\nu^{(M)} = \boldsymbol{E}_i, \tag{12}$$

where,

$$\begin{aligned}
&\boldsymbol{X} \triangleq [(\boldsymbol{Q}_1\boldsymbol{G}_1 + \boldsymbol{Q}_2\boldsymbol{G}_3) - (\boldsymbol{Q}_1\boldsymbol{G}_2 + \boldsymbol{Q}_2\boldsymbol{G}_4)\boldsymbol{Q}_4^{-1}\boldsymbol{Q}_3],\\
&\boldsymbol{A}_\nu^{(M)} \triangleq [A_1^{(M)}, A_2^{(M)}, \cdots, A_{2N_1+1}^{(M)}]^T.
\end{aligned}$$

We derive the other unknown coefficients $A_\nu^{(1)}$, $B_\nu^{(1)}$, $B_\nu^{(M)}$ from solution obtained by solving Eq. (12). As a result, we evaluate the reflection coefficients R_n by using the unknown coefficients. The reflected electric fields $\widetilde{E}_z^{(r)}(x,y)$ in complex frequency domain obtained from second term of Eq. (2) are transformed into the normalized time domain by using the following FILT method:

$$\begin{aligned}
E_z^{(r)}(T) &= \frac{1}{2\pi j}\int_{\gamma - j\infty}^{\gamma + j\infty} \widetilde{E}_z^{(r)}(X,Y)\, e^{ST} dS,\\
&= \frac{e^a}{T}\left(\sum_{n=1}^{N-1} F_n - 2^{-(J+1)}\sum_{L=0}^{J} C_{JL} F_{N+L}\right),
\end{aligned} \tag{13}$$

where,

$$\begin{aligned}
&F_n \triangleq (-1)^n Im\left[\widetilde{E}_z^{(r)}(X,Y)\right],\ S \triangleq \frac{a + j(n-0.5)\pi}{T},\\
&C_{JJ} = 1,\ C_{JL-1} \triangleq C_{JL} + \frac{(J+1)!}{L!(J+1-L)!}.
\end{aligned}$$

N is the truncation mode number of the FILT method, J is the number of terms in the Euler transformation, S ($\triangleq st_w$) is the normalized complex frequency, T ($\triangleq t/t_w$) is the normalized time, and X ($\triangleq x/d_0$), Y ($\triangleq y/p$) are the normalized coordinates.

3. Numerical Results

We employ the dispersive property with soil moisture 5% [15], [16] and constant throughout in this paper. The parameters for the numerical analysis were set as center frequency f_0 = 1GHz ($t_w = 1/f_0$), normalized depth $D_0(\triangleq d_0/p)$ = 0.2, normalized period $P(\triangleq p/(t_w c))$ = 1. In the following analysis, the computational parameters use $a = 4$, $J = 5$, $N = 10$, $M = 10$, and $N_1 = 20$.

Figures 3 (a) and (b) show the waveform of pulse response for reflection electric field $E_z^{(r)}(T)$ of Eq. (2) and normalized magnetic field $H_y^{(r)}(T)$ of Eq. (3) for different $\Delta(\triangleq \delta/p)$ under the medium width $W_p(\triangleq w/p) = 0.5$. Figure 3 (c) shows the differential waveform $f(T)$ ($\triangleq E_z^{(r)}(T) - H_y^{(r)}(T)$) for results of Figs. 3 (a) and (b). From in Fig. 3, we can see the following features:

(1-1) In case of the reflection electric field; the effect of Δ is seen clearly at $0.5 \le T \le 2$ as Δ increase. We can consider the influence is because that propagating velocity of reflected wave for slanted cavity region is fast, and phase and amplitude became large.

(1-2) In case of the reflection magnetic field; the characteristics tendency is the same with reflection electric field. But, the difference between the electric and magnetic fields appears at $1 \le T \le 2$ and $3 \le T \le 4$.

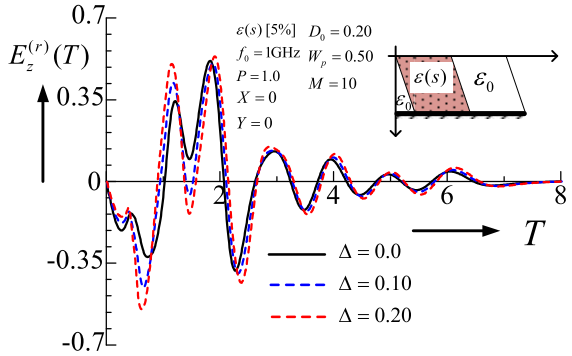

(a) Reflection electric field $E_z^{(r)}(T)$

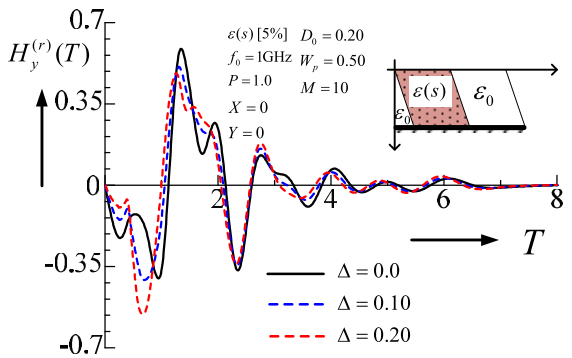

(b) Reflection magnetic field $H_y^{(r)}(T)$

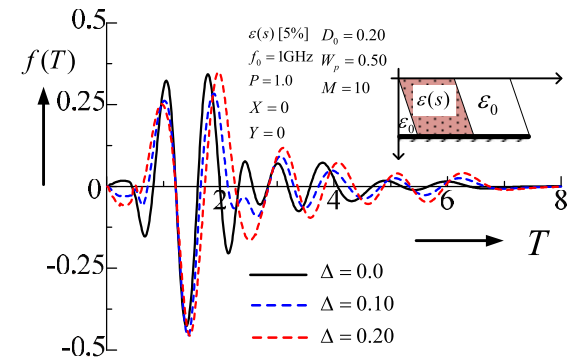

(c) Differential waveform $f(T)$ $\left(\triangleq E_z^{(r)}(T) - H_y^{(r)}(T)\right)$

Fig. 3 Waveform of pulse response for different Δ with $W_p = 0.5$.

We can consider it as the influence of the complex frequency for magnetic field component. In the future, we will analyze the transient scattering problem with arbitrary objects buried in dispersion media. Then, we thought that it is difficult to predict the shape information by using only the electric field component. Therefore, we discuss it to specify influence of the slanted cavity from information of waveform by using both the electric and magnetic fields component in TE wave.

(1-3) From in Fig. 3 (c), the influence of slanted air widths is seen clearly at near $0.0 < T \leq 0.5$ and $2.0 \leq T \leq 3.0$, and other characteristic tendency is about same with the phase delay. We can understand that the result of $\Delta = 0.0$ for Fig. 3 (c) is the different due to the electric and magnetic fields. Consequently, we are considered that it is possible to extract the effect on the width of slanted cavity from further investigation the differential waveform between $\Delta = 0.0$ and $\Delta \neq 0.0$.

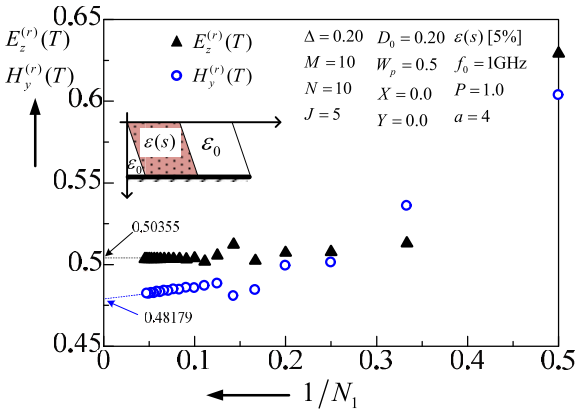

(a) Convergence of truncation mode number $1/N_1$

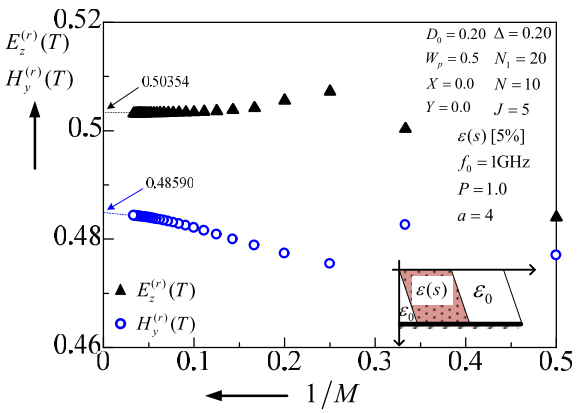

(b) Convergence of multilayer division number $1/M$

Fig. 4 Convergence of $E_z^{(r)}(T)$ and $H_y^{(r)}(T)$ vs. $1/N_1$ and $1/M$.

Next, we confirm the computational accuracy with a convergence test of the truncation mode number $1/N_1$ and multilayer division number $1/M$ as fixed FILT parameters.

Figures 4 (a) and (b) show the convergence of reflection electric and magnetic fields $E_z^{(r)}(T)$, $H_y^{(r)}(T)$ versus $1/N_1$ at $T = 1.15$, $T = 1.26$, respectively for fixed M, and $1/M$ at $T = 1.15$, $T = 1.26$, respectively for fixed N_1 under the same conditions as in Fig. 3. From Fig. 4, it obtained the results of computational accuracy as follows:

(2-1) From Fig. 4 (a), the relative error of $E_z^{(r)}(T)$, $H_y^{(r)}(T)$ to the extrapolated true values are less than about 0.1% when we computed at fixed $M = 10$.

(2-2) From Fig. 4 (b), the relative error of $E_z^{(r)}(T)$, $H_y^{(r)}(T)$ to the extrapolated true values are less than about 0.1% and 1% when we computed at fixed $N_1 = 20$, respectively.

Therefore, we were able to see that our novel method can compute the pulse responses for $E_z^{(r)}(T)$ and $H_y^{(r)}(T)$ to

within 1% and 0.1% degree of the true value with high accuracy when we computed at $M = 10$ and $N_1 = 20$ from these results. And also, we need to see the response $H_y^{(r)}(T)$ at as increase M. In this study, to examine the influence of harmonics for all reflection coefficients R_n, we have investigated the reflected electric and magnetic fields by using the sum of spatial harmonics for a fixed observation point. In the future, we will investigate the pulse response for an influence of only spatial harmonics.

4. Conclusions

In this paper, we analyzed the pulse responses of slanted grating structure in periodically arrayed cavity and dispersion media by using a combination of the FSEM, FILT, and MDM methods, and investigated the influence of slanted air widths on the different waveform of $f(T)$.

As a result, we clarified the influence of both cavity width and the computational accuracy for truncation mode number and multilayer division number.

In the future, we would like to apply present method to pulse response analysis with arbitrary cavity shape.

Acknowledgments

This work was partially supported by JSPS KAKENHI Grant Number JP21K04239.

References

[1] W.T. Hong, S. Kang, W. Han, and J. Lee, "Investigation of ground cavity using ground penetrating radar," Proc. 19th International Conf. Soil Mechanics and Geotechnical Engin., pp.935–938, 2017.
[2] R. Persico, Introduction to Ground Penetrating Radar: Inverse Scattering and Data Processing, Wiley, 2013.
[3] H.M. Jol, "Ground Penetrating Radar Theory and Application," Elesevier, 2009.
[4] M. Nishimoto, K. Nagayoshi, S. Ueno, and Y. Kumura, "Classification of Landmine-Like Objects Buried under Rough Ground Surfaces Using a Ground Penetrating Radar," IEICE Trans. Electron., vol.E90-C, no.2, pp.327–333, 2007.
[5] Y.V. Kang and H.C. Hsu, "Application of ground penetrating radar to identify shallow cavities in a coastal dyke," J. Applied Science and Engineering, vol.16, no.1, pp.23–28, 2013.
[6] X. Wei and Y. Zhang, "Interference Removal for Autofocusing of GPR Data From RC Bridge Decks," IEEE J. App. Earth and Rem. Sens., vol.8, no.3, pp.1145–1151, 2015.
[7] J. Sonoda, T. Kon, M. Sato, and Y. Abe, "Characteristics of Detection for Cavity under Reinforced Concrete Using Ground Penetrating Radar by FDTD Method," IEICE Trans. Electron., vol.J100-C, no.8, pp.302–309, 2017.
[8] H. Liu, B. Xing, J. Zhu, B. Zhou, F. Wang, X. Xie, and Q.H. Liu, "Quantitative Stability Analysis of Ground Penetrating Radar Systems," IEEE Geosci. Remote Sens. Lett., vol.15, no.4, pp.522–526, 2018.
[9] K. Tada and Y. Iwatani, "Electrical technology using for the archaeological exploration," IEEJ Journal, vol.125, no.3, pp.173–176, 2005.
[10] L.B. Felsen Ed., "Topics in Applied Physics: Transient Electromagnetic Fields," vol.10, Springer-Verlag, 1976.
[11] T. Tanaka, T. Takenaka, and S. He, "An FDTD approach to the time-domain inverse scattering problem for an inhomogeneous cylindrical object," Microwave and Optical Tech., Lett., vol.20, no.1, pp.72–77, 1999.
[12] P. Shangguan and I.L. Al-Qadi, "Calibration of FDTD Simulation of GPR Signal for Asphalt Pavement Compaction Monitoring," IEEE Trans. Geosci. Remote Sens., vol.53, no.3, pp.1538–1548, 2015.
[13] M. Sato, "Subsurface Imaging by Ground Penetrating Radar," IEICE Trans. Electron., vol.J85-C, no.7, pp.520–530, 2002.
[14] M. Sato, "Social Contributions by Subsurface Electromagnetic Survey," IEICE Trans. Electron., vol.J103-C, no.3, pp.186–193, 2020.
[15] R. Ozaki, N. Sugizaki, and T. Yamasaki, "Numerical Analysis of Pulse Responses in the Dispersion Media," IEICE Trans. Electron., vol.E97-C, no.1, pp.45–49, 2014.
[16] J.E. Hipp, "Soil electromagnetic parameters as functions of frequency, soil density, and soil moisture," Proc. IEEE, vol.62, no.1, pp.98–103, 1974.
[17] T. Hinata and T. Hosono, "On the scattering of electromagnetic wave by plane grating placed in homogeneous medium – mathematical foundation of point matching method and numerical analysis," IEICE Trans. Japan, vol.J59-B, no.12, pp.571–578, 1976.
[18] T. Hosono, "Numerical Inversion of Laplace Transform and some Applications to Wave Optics," Radio Science, vol.16, no.6, pp.1015–1019, 1981.
[19] T. Hosono, "International series of monographs on advanced electromagnetic: FILT," vol.2, Science House Inc., 2013.
[20] S. Ohnuki, "Time-Domain Analysis of Electromagnetic Waves Using Fast Inverse Laplace Transform," IEICE Trans. Electron., vol.J103-C, no.4, pp.203–210, 2020.
[21] R. Ozaki and T. Yamasaki, "Analysis of Pulse Reflection Responses from Periodic Perfect Conductor in Two Dispersion Media," IEICE Trans. Electron., vol.E100-C, no.1, pp.80–83, 2017.
[22] R. Ozaki and T. Yamasaki, "Analysis of Pulse Responses from Conducting Strips with Dispersion Medium Sandwiched Air Layer," IEICE Electron. Express, vol.15, no.6, pp.1–6, 2018.
[23] R. Ozaki, T. Kagawa, and T. Yamasaki, "Analysis of Pulse Responses by Dispersion Medium with Periodically Conducting Strips," IEICE Trans. Electron., vol.E103-C, no.11, pp.613–616, 2020.
[24] R. Ozaki and T. Yamasaki, "Pulse Responses from Periodically Arrayed Dispersion Media with an Air Region," IEICE Trans. Electron., vol.E102-C, no.6, pp.479–486, 2019.
[25] T. Yamasaki and H. Tanaka, "Scattering of electromagnetic waves by a dielectric grating with planar slanted-fringe," IEICE Trans. Electron., vol.E76-C, no.10, pp.1435–1442, 1993.
[26] H. Tanaka, T. Yamasaki, and T. Hosono, "Propagation characteristics of dielectric waveguides with slanted grating structure," IEICE Trans. Electron., vol.E77-C, no.11, pp.1820–1827, 1994.
[27] K. Watanabe, "Electromagnetic Scattering from Slanted grating," Proc. IEICE General Conf., CS-1-1, pp.1–2, 2016. (in Japanese)
[28] H. Wakabayashi, M. Asai, and J. Yamakita, "Three-dimensional analysis of structural coloration by a slanted dielectric grating," J. Optical Society of Am. A., vol.37, no.10, pp.1539–1547, Oct. 2020.
[29] R. Ozaki and T. Yamasaki, "Analysis of Pulse Responses by Dispersion Media with Slanted Air Region," IEICE Technical Report, EMT2020-38, pp.59–63, Nov. 2020.
[30] R. Ozaki and T. Yamasaki, "Analysis of Pulse Responses by Dispersion Media with Slanted Air Region —An Influence of the Magnetic Fields in TE case—," Proc. IEICE General Conf., C-1-6, 2021. (in Japanese)
[31] R. Ozaki and T. Yamasaki, "Propagation Characteristics of Dielectric Waveguides with Arbitrary Inhomogeneous Media along the Middle Layer," IEICE Trans. Electron., vol.E95-C, no.1, pp.53–62, 2012.
[32] R. Ozaki and T. Yamasaki, "Energy Distribution of Periodically Dielectric Waveguides by Arbitrary Shape of Dielectric Constants —The Influence of Dielectric Structures in the Middle Layer—," IEICE Trans. Electron., vol.E99-C, no.7, pp.820–824, 2016.